ISSN 1063-7834, Physics of the Solid State, 2010, Vol. 52, No. 1, pp. 167–175. © Pleiades Publishing, Ltd., 2010.
Original Russian Text © M.V. Gorev, E.V. Bogdanov, I.N. Flerov, A.G. Kocharova, N.M. Laptash, 2010, published in Fizika Tverdogo Tela, 2010, Vol. 52, No. 1, pp. 156–164.

LATTICE DYNAMICS AND PHASE TRANSITIONS

Investigation of Thermal Expansion, Phase Diagrams, and Barocaloric Effect in the $(NH_4)_2WO_2F_4$ and $(NH_4)_2MoO_2F_4$ Oxyfluorides

M. V. Gorev[a, b, *], E. V. Bogdanov[a], I. N. Flerov[a, b], A. G. Kocharova[a], and N. M. Laptash[c]

[a] *Kirensky Institute of Physics, Siberian Branch, Russian Academy of Science, Akademgorodok 50, Krasnoyarsk, 660036 Russia*

* *e-mail: gorev@iph.krasn.ru, flerov@iph.krasn.ru*

[b] *Siberian Federal University, pr. Svobody 79, Krasnoyarsk, 660041 Russia*

[c] *Institute of Chemistry, Far Estern Branch, Russian Academy of Sciences, ul. Stoletiya Vladivostoka 159, Vladivostok, 690022 Russia*

Received April 28, 2009; in final form, June 9, 2009

Abstract—The thermal expansion along the principal crystallographic axes of the $(NH_4)_2WO_2F_4$ and $(NH_4)_2MoO_2F_4$ oxyfluorides has been studied. The anomalous behavior of $\alpha_i(T)$ due to the phase transitions has been revealed at $T_1 = 271.4$ K and $T_2 \approx 180$ K for the molybdate and at $T_1 = 201.5$ K and $T_2 \approx 161$ K for the tungstate. The quantities dT/dp and $dT/d\sigma_i$, which characterize the dependence of the phase transition temperatures on the hydrostatic and uniaxial pressures, have been determined from analyzing the results of studies of the thermal expansion and heat capacity with the use of the Pippard relations. The $p-T$ and σ_i-T phase diagrams reflect different characters of the influence of the pressure on the stability of the initial and distorted phases of the oxyfluorides. The magnitudes of the extensive and intensive barocaloric effects determined in the vicinity of the structural phase transitions are as follows: ΔS_{BCE} varies from approximately -10 to -17 J/mol K and $\Delta T_{AD} \approx 8-17$ K for the molybdate and ΔS_{BCE} varies from approximately -10 to -17 J/mol K and $\Delta T_{AD} \approx 8-13$ K for the tungstate.

DOI: 10.1134/S1063783410010294

1. INTRODUCTION

Interest in compounds with structures that contain distorted octahedral ionic groups $|MO_xF_{6-x}|$ ($x = 1, 2, 3$) with ions M displaced from the center of octahedra, as a rule, is related to the search for the criteria of the design of noncentrosymmetric materials exhibiting ferroelectric, piezoelectric, and pyroelectric properties. However, the majority of these compounds crystallize in centrosymmetric space groups due to the orientational disordering of structural units. To develop polar materials, it is necessary to understand the nature of the orientational disorder of oxyfluoride anions and to prevent both the ordering of oxygen and fluoride ligands in the anion and the centrosymmetric arrangement of octahedral anions in the crystal lattice with respect to each other.

In the case of oxyfluorides with ionic groups $|MO_xF_{6-x}|^{2-}$ ($x = 2$, $M = Mo^{6+}$, W^{6+}), compounds with organic and hybrid organic–inorganic cations have been investigated most extensively [1, 2]. In inorganic compounds $A_2MO_2F_4$ [3–7], anions are disordered in all cases, except for $Na_2WO_2F_4$ [3] and $K_2MoO_2F_4$ [4]. Unfortunately, for the most part, studies have been carried out only at room temperature, and information on phase transitions in these compounds is absent. However, investigations into the orientational ordering of ionic groups due to the phase transitions can provide additional information and favor the design of polar compounds with desired properties.

The search and study of phase transitions in the series of $A_2MO_2F_4$ oxyfluorides have been recently performed only for ammonium compounds. At room temperature, the $(NH_4)_2WO_2F_4$ and $(NH_4)_2MoO_2F_4$ crystals have an orthorhombic structure $G_0 = Cmcm$ ($Z = 4$) [7–10] and, as the temperature decreases, sequentially undergo two phase transitions $G_0 \longrightarrow G_1 \longrightarrow G_2$ at temperatures T_1 and T_2 [8–15]. The former structural transformation is an order–disorder first-order transition with a significant change in the entropy $\Delta S_1 \approx R\ln 8 - R\ln 9$ [9, 11, 15]. A substantially smaller change in the entropy upon the latter transition in both oxyfluorides ($\Delta S_2 \approx 0.15R$) has been attributed to a displacive phase transition.

In spite of the small difference between the ionic radii of molybdenum and tungsten and the same sym-

metry of the initial G_0 phases, there are significant differences between the phase transition temperatures, symmetries of the distorted phases, and properties of the $(NH_4)_2WO_2F_4$ and $(NH_4)_2MoO_2F_4$ compounds. The structure of the distorted G_1 phase of the tungstate is triclinic ($P\bar{1}$, $Z = 4$) [7], whereas the molybdate structure is orthorhombic (*Pnma*, $Z = 4$) [10]. In both oxyfluorides, there are no noticeable differences between the structures of the intermediate (G_1) and low-temperature (G_2) distorted phases. As a result of the Mo $\longrightarrow$ W substitution, the initial *Cmcm* phase becomes less stable to variations in external parameters (temperature and pressure), which manifests itself in a significant increase in the temperature T_1 and an anomalously large pressure coefficient dT_1/dp [15] considerably exceeding that determined for $(NH_4)_2WO_2F_4$ [9]. However, the range of existence of the intermediate phase is substantially extended from 40 to 90 K due to the significantly smaller change in T_2.

The analysis of the structure and entropy of the phase transitions [15] allowed us to propose a model of high-temperature transitions in the tungstate and molybdate and to relate significant changes in the entropy to the ordering of the ammonium groups and also to the ordering (complete in $(NH_4)_2WO_2F_4$ and partial in $(NH_4)_2MoO_2F_4$) of the fluorine–oxygen octahedra.

The nature of the phase transitions in the oxyfluorides under study was determined to be nonferroelectric [15]. Therefore, the pressure is the main external parameter that makes it possible to change the temperature and sequence of structural distortions. The $p-T$ phase diagram of $(NH_4)_2WO_2F_4$ was experimentally obtained in our earlier work [9]. The temperatures of both phase transitions increase nonlinearly with an increase in the pressure; in this case, $dT_1/dp < dT_2/dp$. This means that an increase in the hydrostatic pressure leads to a decrease in the range of existence of the intermediate phase. No triple points and pressure-induced phases were revealed up to 0.5 GPa. However, the character of the dependences $T_i(p)$ suggests the disappearance of the intermediate distorted phase and existence of the triple point near 0.7 GPa. In $(NH_4)_2MoO_2F_4$) under pressure, the phase transition was revealed only at T_1 with the pressure coefficient $dT_1/dp = 92.8$ K/GPa [15].

A very high degree of disordering of the ionic groups in the high-symmetry phases of the oxyfluorides and their ordering as a result of single or successive phase transitions accompanied by significant changes in the entropy up to $\Delta S \geq R\ln 8$ and also a considerable sensitivity to the external pressure make these materials promising from the standpoint of manifestation of substantial caloric effects in them.

In recent years, caloric effects of different physical natures in solids and cooling devices based on them have attracted more and more attention of researchers [16, 17]. Generally speaking, these effects are associated with the change in the entropy and temperature of a thermodynamic system with a change in generalized external fields (electric, magnetic) during isothermal and adiabatic processes, respectively. It is quite obvious that, apart from magnetic and electric fields, hydrostatic pressure or uniaxial (compressive or tensile) mechanical stresses can influence the entropy of the thermodynamic system and cause the barocaloric (BCE) or piezocaloric (PCE) effects.

The entropy of a solid is a sum of entropies of different subsystems, such as the lattice (S_L), electronic (S_e), magnetic (S_M), and electric (S_{EL}) entropies, as well as the anomalous entropy related to phase transitions (ΔS_{an}). All the above types of entropies depend, to some degree, on the external pressure, and their variations can contribute to the barocaloric effect. The study of the barocaloric effect in the range of structural phase transitions by Müller et al. [18] in $Pr_{1-x}La_xNiO_3$ solid solutions should be considered a priority work. The barocaloric effect was also studied in materials with other physical mechanisms of a change in the entropy under pressure [19–23]. In some cases, the extensive (ΔS_{BCE}) and intensive (ΔT_{AD}) barocaloric effects at pressures of lower than 1 GPa appeared to be fairly strong and comparable to variations in ΔS and ΔT in the magnetocaloric effect [19, 20].

It is evident that the higher the degree of disordering of structural units in the initial high-temperature phase of a material, the higher the probability of occurrence of an order–disorder phase transition with a decrease in the temperature; in this case, a significant barocaloric effect can manifest itself in the vicinity of the temperature of this transition.

In this work, the thermal expansion of the $(NH_4)_2WO_2F_4$ and $(NH_4)_2MoO_2F_4$ crystals were studied in order to obtain additional information on the phase transitions, to determine the thermodynamic parameters, and to elucidate the type of the $p-T$ (hydrostatic pressure–temperature) and $\sigma-T$ (uniaxial pressure–temperature) phase diagrams. Moreover, we determined the magnitudes of the intensive and extensive barocaloric and piezocaloric effects from the data on the temperature dependence of the heat capacity at atmospheric pressure and those obtained in the study of the $p-T$ and $\sigma-T$ phase diagrams.

2. SAMPLE PREPARATION AND EXPERIMENTAL TECHNIQUE

Relatively large single crystals of $(NH_4)_2WO_2F_4$ and $(NH_4)_2MoO_2F_4$ in the form of prisms or thick plates were grown from solutions in the course of slow evaporation in air according to the techniques described in [8, 13]. The samples for dilatometric

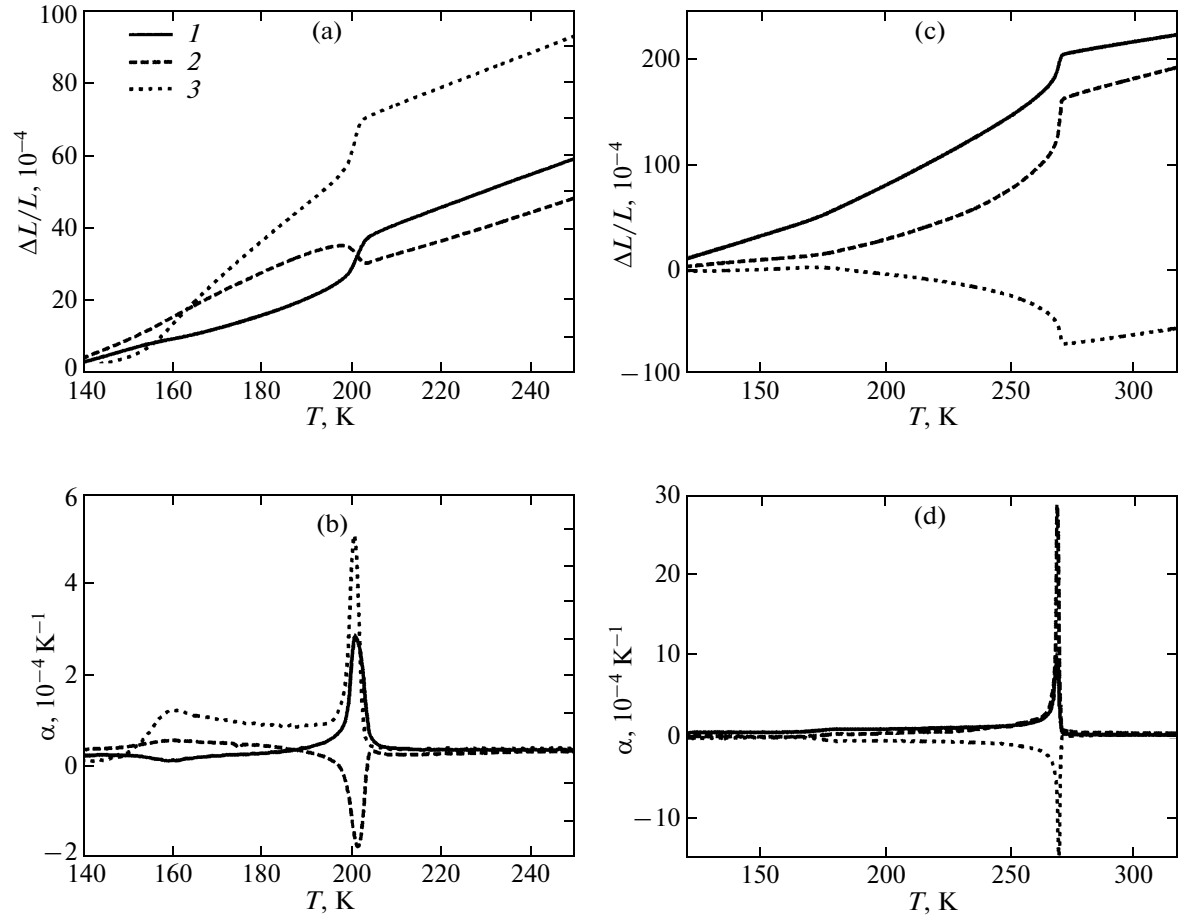

Fig. 1. Temperature dependences of (a, c) the strain $\Delta L/L$ and (b, d) the linear thermal expansion coefficient α along the (*1*) *a*, (*2*) *b*, and (*3*) *c* crystallographic directions for (a, b) $(NH_4)_2WO_2F_4$ and (c, d) $(NH_4)_2MoO_2F_4$.

measurements were prepared in the form of parallelepipeds 5.080, 10.108, and 2.385 mm in size for $(NH_4)_2WO_2F_4$ and 7.892, 1.579, and 2.843 mm in size for $(NH_4)_2MoO_2F_4$ along the *a*, *b*, and *c* crystallographic directions, respectively.

The thermal expansion was measured on a NETZSCH DIL-402C dilatometer in the temperature range 140–320 K in the dynamic mode at a heating rate of 3 K/min. Fused silica reference samples were used for calibrating and including the expansion of the measurement system.

3. RESULTS

3.1. Thermal Expansion

The temperature dependences of the strain $\Delta L/L$ and the linear thermal expansion coefficients along three crystallographic directions *a*, *b*, and *c* for $(NH_4)_2WO_2F_4$ and $(NH_4)_2MoO_2F_4$ are shown in Fig. 1. For each direction, we performed several series of measurements, and their results agree satisfactorily with each other. Anomalous behaviors of $\alpha(T)$ at $T_1 =$ 201.5 K and $T_2 \approx 161$ K for $(NH_4)_2WO_2F_4$ and at $T_1 =$ 271.4 K and $T_2 \approx 180$ K for $(NH_4)_2MoO_2F_4$ are due to the phase transitions revealed in [8–15]. The transition temperatures are somewhat higher than those obtained in the measurements of the heat capacity on an adiabatic calorimeter [9, 15] which is associated with the dynamic character of measurements on the dilatometer.

As was expected reasoning from the structural data on the difference between the symmetries of the distorted phases, the behavior of the thermal expansion in $(NH_4)_2WO_2F_4$ and $(NH_4)_2MoO_2F_4$ differs substantially. As the temperature decreases, the strain $\Delta L_a/L_a$ decreases at T_1 for both crystals, $\Delta L_b/L_b$ increases for $(NH_4)_2WO_2F_4$ and decreases for $(NH_4)_2MoO_2F_4$, and $\Delta L_c/L_c$, by contrast, decreases for the tungstate and increases for the molybdate. In spite of this fact, the characters of changes in the volume $\Delta V/V$ and the volume thermal expansion coefficient $\beta = \alpha_a + \alpha_b + \alpha_c$ for both crystals are qualitatively similar and mainly determined by the behavior of the thermal expansion

along the c axis for $(NH_4)_2WO_2F_4$ and along the b axis for $(NH_4)_2MoO_2F_4$.

To separate and analyze the anomalous contribution to the strain, it is necessary to adequately describe the nonanomalous contributions to the strain and the thermal expansion coefficients. We estimated these contributions using two methods for approximating the lattice component of $\Delta V/V$. In the traditional approach, when the elongation at temperatures $T > T_1$ is approximated by a linear dependence, the anomalous contribution to the strain, as a rule, is overestimated and depends on the temperature range in which the approximation is performed. Moreover, the temperature dependences $\Delta L/L(T)$ investigated in our work are clearly nonlinear, and the thermal expansion coefficients $\alpha(T)$ are not constant.

As the temperature decreases, the thermal expansion coefficients should tend to zero and, in the low-temperature range ($T < T_i < \Theta_D$), it is necessary to take into account the relation between the thermal expansion and the heat capacity and the temperature dependence of the heat capacity if only in terms of the Debye model. However, fairly narrow temperature ranges possible for the processing of the nonanomalous behavior of the thermal expansion above T_1 (280–320 K for the molybdate and 220–270 K for the tungstate) complicate this analysis. Therefore, we restricted ourselves to the assumption that, at $T > T_1$, the coefficients $\alpha(T)$ depend almost linearly on the temperature. This approximation significantly improves the approximation of the experimental temperature dependences of $\alpha(T)$ and strain at $T > T_1$ and allows us to estimate the volume jumps upon first-order phase transitions. It is natural that the error in the separation of the anomalous contribution increases with a decrease in the temperature below T_1 in the low-temperature range.

3.2. The Clapeyron–Clausius and Pippard Relations

In [15], the study of the pressure–temperature phase diagrams for the molybdate made it possible to fix only the phase boundary of $G_0 \longrightarrow G_1$. The presence of the data on the heat capacity [9, 15] and thermal expansion allows us to calculate the shift in the transition temperatures under the influence of hydrostatic and uniaxial pressures and to construct the complete phase diagrams.

In the case of the first-order phase transitions at T_0, we can use the Clapeyron–Clausius relation

$$\frac{dT_0}{dp} = \frac{\delta V}{\delta S}, \quad (1)$$

where δV and δS are the volume and entropy jumps at the transition point, respectively. However, the phase transitions at T_1 in both compounds are fairly close to the tricritical point [9, 15]. Moreover, near the phase transition temperatures, the anomalies of the heat capacity and thermal expansion are smeared due to the imperfection of the samples and the dynamic character of the measurements of the thermal expansion. Therefore, the determination of the entropy and volume jumps at T_1 is substantially complicated and associated with the large error. The approximate estimates lead to the values of $dT_1/dp \approx 17$ K/Pa for the tungstate and $dT_1/dp \approx 74$ K/Pa for the molybdate.

In order to determine more accurately dT_1/dp and dT_2/dp, we used the Pippard relations [24], which relate the heat capacity and thermal expansion coefficients near the phase transition temperature; that is,

$$C_p = \frac{V_m T_0}{\gamma_i}\alpha_i + \text{const}, \quad C_p = \frac{V_m T_0}{\gamma}\beta + \text{const}, \quad (2)$$

where C_p is the heat capacity, V_m is molar volume,

$$\gamma_i = \frac{dT_0}{d\sigma_i}, \quad \gamma = \frac{dT_0}{dp} = \sum_i \gamma_i. \quad (3)$$

Relations (2) allow us to determine the shift in the transition temperature under the hydrostatic pressure dT_0/dp and under the influence of uniaxial stresses $dT_0/d\sigma$ and to construct the σ_i–T phase diagrams.

Since the quantities dT/dp and $dT/d\sigma$ and the fulfillment of relations (2) are strongly dependent on the accuracy in the coincidence of the data in temperature near the phase transitions, small discrepancies between the temperature scales in the measurements of the heat capacity on the adiabatic calorimeter (temperature sensor is a platinum resistance thermometer) and the thermal expansion on the dilatometer (thermocouple) will bring about significant errors in the results of the calculation. In this respect, the data on the thermal expansion and heat capacity were reduced to the same temperature scale by bringing the phase transition temperatures into coincidence. The molar volumes were determined from the structural data [7, 9, 13].

The results of the joint processing of the data on the heat capacity and volume thermal expansion coefficients for the distorted phases of $(NH_4)_2WO_2F_4$ near the temperatures T_1 and T_2 are presented in Fig. 2. The Pippard relations (2) are fairly well satisfied for both phase transitions. The deviations from relations (2) are observed at a sufficient distance from the phase transition temperatures $T_1 - T \gtrsim 15$ K and $T_2 - T \gtrsim 15$ K and in the immediate vicinity of the transformations $T_1 - T \lesssim 1.5$ K and $T_2 - T \lesssim 3.5$ K, where the effect of the sample imperfection, the dynamic character of measurements of the thermal expansion, and insufficient accuracy in the coincidence of the temperature scales of the data arrays $C_p(T)$ and $\alpha(T)$ are most significant. A similar behavior of the thermal expansion and heat capacity is also observed for $(NH_4)_2MoO_2F_4$.

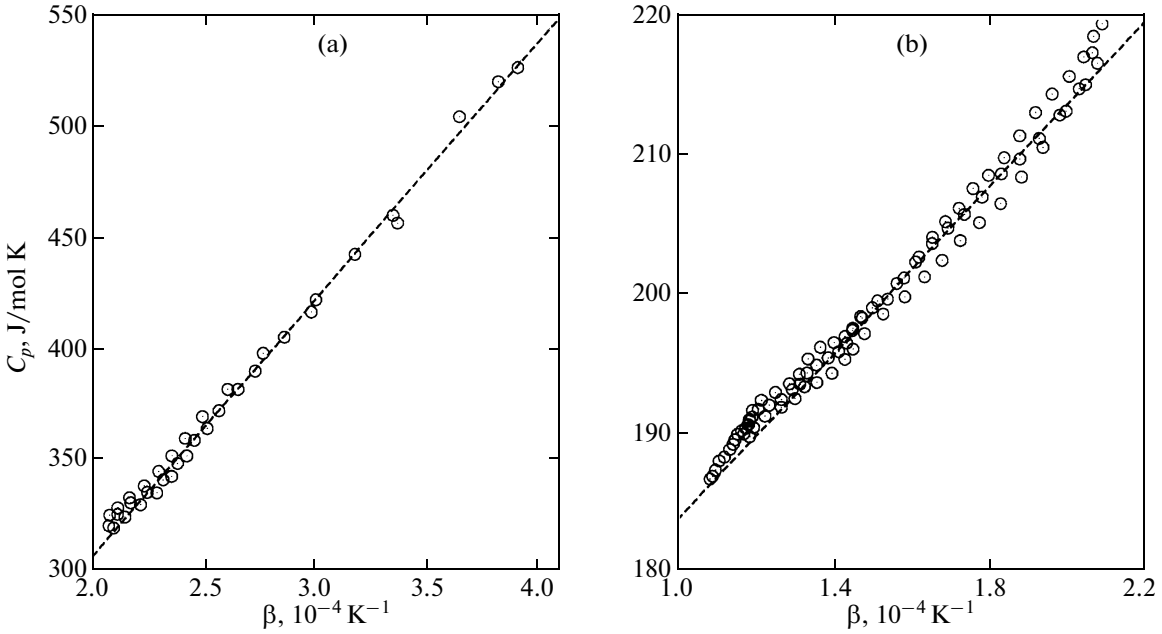

Fig. 2. Dependences of the molar heat capacity on the volume thermal expansion coefficient β below (a) T_1 and (b) T_2 for $(NH_4)_2WO_2F_4$.

The experimental pressure coefficients of the phase transition temperatures and those calculated from the Pippard relations (2) $\gamma = dT/dp$ and $\gamma_i = dT/d\sigma_i$ for both oxyfluorides are listed in Table 1. For the tungstate, the experimental pressure coefficients dT_1/dp and dT_2/dp [9] agree satisfactorily with the values obtained from analyzing the data on the heat capacity and volume and linear thermal expansion coefficients. These facts and good agreement between the experimental and calculated values of dT_1/dp for the molybdate (Table 1) allow us to hope that, for this crystal, we also fairly accurately calculated the value of dT_2/dp, which was not determined experimentally [15].

The values of $dT_1/d\sigma_i$ and $dT_2/d\sigma_i$ are also presented in Table 1.

3.3. Phase Diagrams

The calculated values of dT/dp and $dT/d\sigma$ allow the construction of the $p-T$ phase diagrams (Fig. 3). The experimental data taken from [9, 15] are also presented in Fig. 3. It is worth noting that the temperatures T_1 determined for the tungstate in calorimetric, optical, and dilatometric studies and from differential thermal analysis (DTA) data agree well with each other. However, the temperature T_2 obtained from the DTA measurements is 12–15 K higher than that determined from the measurements of the heat capacity and thermal expansion, which according to [9] is related to the effect of high rates of variation in the temperature during the DTA measurements on the temperature T_2 and to possible uniaxial stresses arising when the sample is cemented to the junction of the differential thermocouple.

Table 1. Experimental pressure coefficients of the temperatures of the $G_0 \longrightarrow G_1$ and $G_1 \longrightarrow G_2$ phase transitions [9, 15] and the corresponding coefficients calculated using the Pippard relations (2)

Pressure coefficient	$(NH_4)_2WO_2F_4$				$(NH_4)_2MoO_2F_4$			
	$G_0 \longrightarrow G_1$		$G_1 \longrightarrow G_2$		$G_0 \longrightarrow G_1$		$G_1 \longrightarrow G_2$	
	experiment	calculation	experiment	calculation	experiment	calculation	experiment	calculation
γ, K/GPa	13.4	15.9	41.7	48.8	92.8	98.6	–	16.7
$\gamma_a + \gamma_b + \gamma_c$, K/GPa	–	16.1	–	53.4	–	98.5	–	17.1
γ_a, K/GPa	–	8.5	–	–5.6	–	52.9	–	21.3
γ_b, K/GPa	–	–10.0	–	9.9	–	93.5	–	18.0
γ_c, K/GPa	–	17.6	–	49.1	–	–47.9	–	–22.2

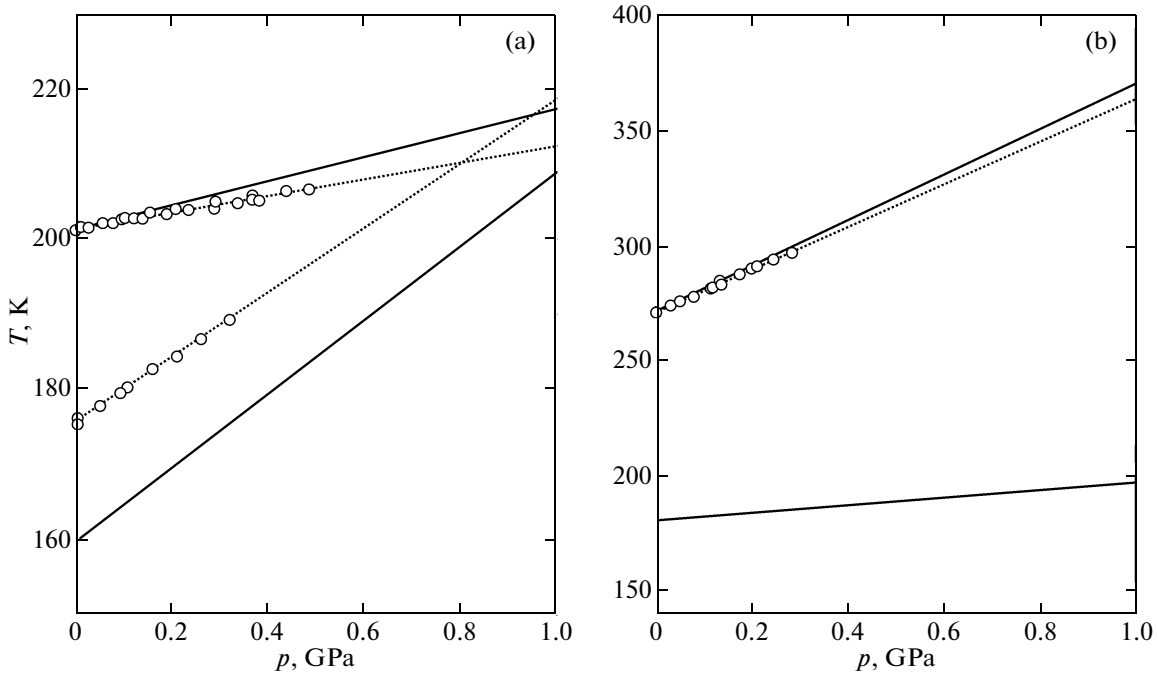

Fig. 3. The $p-T$ phase diagrams for (a) $(NH_4)_2WO_2F_4$ and (b) $(NH_4)_2MoO_2F_4$. Points and dotted lines indicate the experimental data taken from [9, 15]. Solid lines represent the results of the calculations with the use of the Pippard relations.

As can be seen from Table 1, the substitution of molybdenum for tungsten brings about a significant increase in dT_1/dp and a decrease in dT_2/dp by a factor of three, which leads to an increase in the temperature range of stability of the G_1 phase with increasing pressure.

The uniaxial stresses along the c axis in the tungstate and along the b axis in the molybdate almost do not change the form of the $\sigma-T$ phase diagrams as compared to the $p-T$ diagrams, which follows from the values of the pressure coefficients (Table 1). Radical changes in the phase diagram for the tungstate are associated only with the stress along the a axis. In this case, the temperature range of stability of the G_1 phase increases with increasing σ_a ($dT_1/d\sigma_a > dT_2/d\sigma_a$). In the molybdate, the stress σ_c brings about the change in signs of $dT_1/d\sigma_c$ and $dT_2/d\sigma_c$ and a decrease in the range of stability of the G_1 phase ($dT_1/d\sigma_c < dT_2/d\sigma_c$).

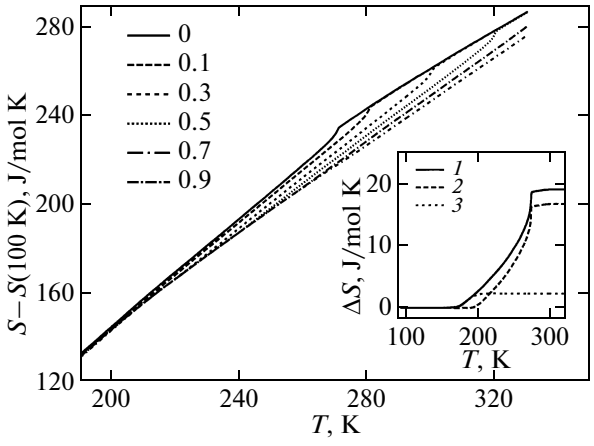

Fig. 4. Temperature dependences of the entropy of $(NH_4)_2MoO_2F_4$ at different pressures. Numbers are the pressures (in GPa). The inset shows the temperature dependences of the anomalous entropy components (*1*) ΔS, (*2*) ΔS_1, and (*3*) ΔS_2 at $p = 0$.

4. BAROCALORIC AND PIEZOCALORIC EFFECTS

The intensive and extensive barocaloric and piezoelectric effects in $(NH_4)_2WO_2F_4$ and $(NH_4)_2MoO_2F_4$ were determined in the same manner, as was done for $EuNi_2(Si_{0.15}Ge_{0.85})_2$ [20], with the use of the data on the heat capacity at atmospheric pressure [9, 15] and the $p-T$ and σ_i-T phase diagrams obtained in our work.

Since ionic bonds are dominant in the oxyfluoride crystals, it is reasonable to assume that the pressure predominantly affects the phase transition entropy. Substantial changes in the other entropy components, including the lattice entropy, are most likely almost absent in the range of relatively low pressures under study. Thus, the lattice entropy determined at atmospheric pressure can be used as a background entropy when analyzing the results of the pressure effect.

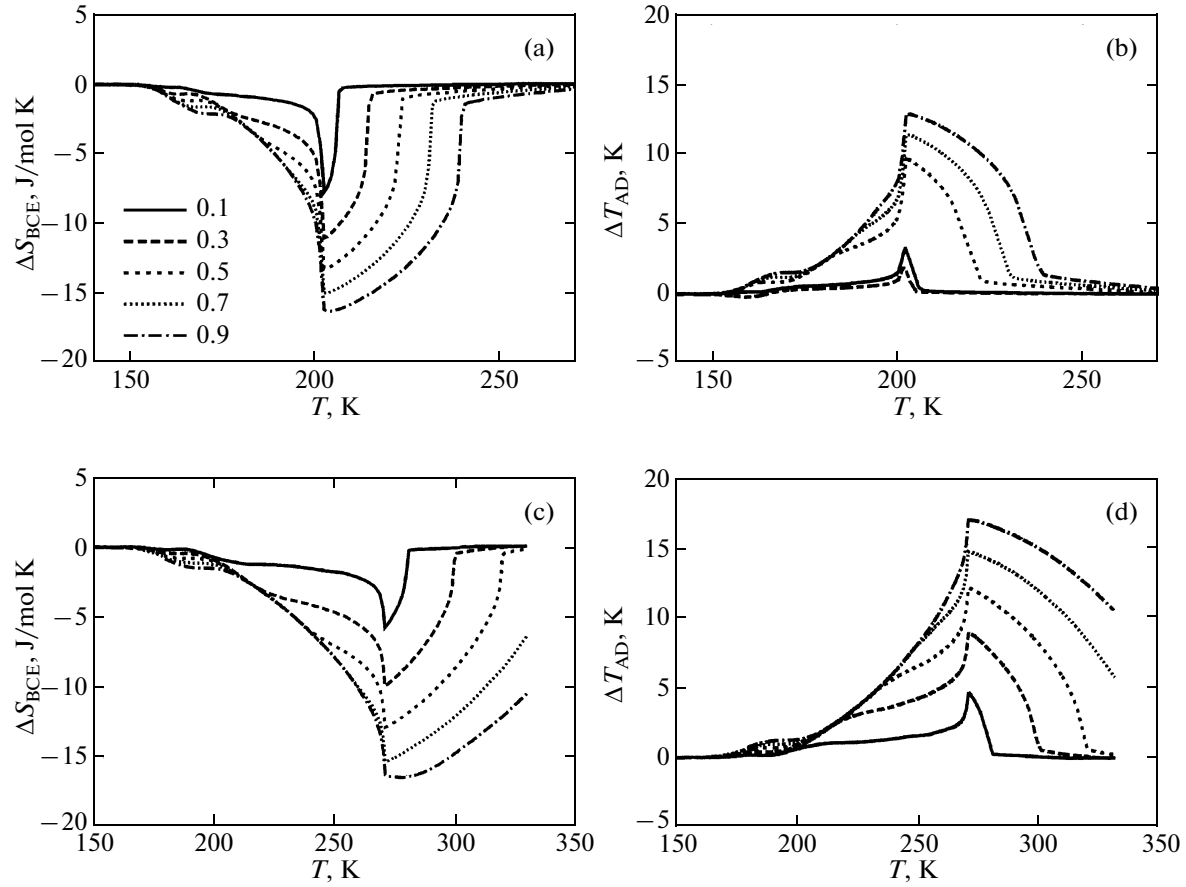

Fig. 5. (a, c) Extensive and (b, d) intensive caloric effects in (a, b) $(NH_4)_2WO_2F_4$ and (c, d) $(NH_4)_2MoO_2F_4$ according to the calculations from the data on the heat capacity and dT/dp at different pressures. Numbers are the pressures (in GPa).

The lattice component of the heat capacity $C_L(T)$ was determined by approximating the data outside the range of existence of the anomalous contribution with the use of a combination of the Debye and Einstein functions. The temperature dependences of the change in the lattice entropy in the temperature range of the measurements $S_L(T) - S_L(100\ \text{K})$ and the anomalous components of $\Delta S(T)$ were obtained by integrating the functions $C_L(T)/T$ and $(C_p(T) - C_L(T))/T$, respectively, which behave identically in both crystals. The calculated results for $(NH_4)_2MoO_2F_4$ are presented in Fig. 4. The anomalous entropies of the phase transitions at T_1 and T_2 were separated using the approximation of the data near T_2 by the sigmoid $\Delta S_2(T) = a/(1 + \exp[(T_2 - T)/b])$ (inset to Fig. 4).

The change in the total entropy of the crystals as functions of the temperature and pressure was determined by summing up the lattice component of the entropy $S_L(T)$ (independent of the pressure) and the anomalous entropy components $\Delta S_1(T)$ and $\Delta S_2(T)$ shifted in temperature for each pressure according to the dependences $T_1(p)$ and $T_2(p)$ (Table 1, Fig. 3). In this case, it was assumed that, in the pressure range under investigation, the hydrostatic pressure does not lead to a substantial change in the degree of closeness of the phase transition to the tricritical point and, hence, does not change the dependence of the anomalous heat capacity. The pressure also does not change the quantities ΔS_i, because it does not change the number of possible states for ordering units before and after the transition. It is assumed that the quantity ΔS_2 also remains unchanged under pressure.

The magnitudes of the extensive barocaloric effect determined as $\Delta S_{BCE}(T, p) = S(T, p) - S(T, 0)$ for $(NH_4)_2WO_2F_4$ and $(NH_4)_2MoO_2F_4$ are presented in Figs. 5a and 5c, respectively. The magnitudes of the intensive barocaloric effect ΔT_{AD} obtained from the condition $S(T, 0) = S(T + \Delta T_{AD}, p)$ are presented in Figs. 5b and 5d.

The caloric effects under uniaxial stresses were calculated in the same manner. In this case, the dependence of the total entropy of the sample on the temperature and stress was determined by summing up the lattice component of the entropy $S_L(T)$ and the anomalous entropy components $\Delta S_1(T)$ and $\Delta S_2(T)$ shifted

Table 2. Phase transition temperatures T_0 and caloric effects ΔT_{AD} and ΔS_{CE} induced by the magnetic fields ΔH, electric fields ΔE, and hydrostatic pressure p

Material	T_0, K	ΔT_{AD}, K	ΔS_{CE}, J/kg K	ΔH, kOe	ΔE, kV/cm	p, GPa	References
$(NH_4)_2MoO_2F_4$	270	~12	~50			0.5	
$(NH_4)_2WO_2F_4$	201	~10	~40			0.5	
CeSb	16	4	19			0.2–0.5	[20]
$EuNi_2(Si_{0.15}Ge_{0.85})_2$	50	14	39			0.2–0.5	[20]
MnAs	312	13	32	50			[16]
$Gd_5Si_2Ge_2$	280	15	18.5	50			[25]
PST	290	2.4			138		[26]
PZT	500	15	8		480		[27]

Note: PST is $PbSc_{1/2}Ta_{1/2}O_3$, and PZT is $PbZr_{0.95}Ti_{0.05}O_3$ (300-nm film).

in temperature for given mechanical stresses according to the dependences $T_1(\sigma)$ and $T_2(\sigma)$ obtained from the Pippard relations (Table 1). It was assumed that the uniaxial stresses, like the hydrostatic pressure, do not substantially change the degree of closeness of the phase transitions to the tricritical point.

Unlike the hydrostatic pressure, the mechanical stresses along the b axis in $(NH_4)_2WO_2F_4$ and along the c axis in $(NH_4)_2MoO_2F_4$ change the sign of the caloric effects at T_1 due to the change in the signs of the pressure coefficients $dT_1/d\sigma$ along these directions as compared to dT_1/dp (Table 1).

In the tungstate, the strongest effects are observed when the stresses are applied along the c direction (at $\sigma_c = 9$ GPa, the quantities ΔS_{PCE} and ΔT_{AD} are as large as 14 J/mol K and 8 K, respectively). The pressure coefficients for this crystal, when the stresses are applied along the a and b directions, are relatively small (Table 1), which brings about small magnitudes of the caloric effects ($\Delta S \approx -10$ J/mol K, $\Delta T \approx +5$ K at $\sigma_a = 9$ GPa and $\Delta S \approx +10$ J/mol K, $\Delta T \approx -5$ K at $\sigma_b = 9$ GPa) and narrow temperature ranges of their existence (170–200 K). The extensive and intensive piezocaloric effects in the molybdate are considerably stronger than those in the tungstate, especially when the stresses are applied along the b direction (at $\sigma_b = 9$ GPa, ΔS_{PCE} and ΔT_{AD} are as large as ~17 J/mol K and 15 K, respectively); moreover, the effects are observed over a wider temperature range (270–350 K).

It is of interest to compare the data obtained on the intensive and extensive barocaloric effects in the oxyfluorides near the structural phase transitions with the parameters of the magnetocaloric and electrocaloric effects in some materials that undergo transitions to the ferromagnetic and ferroelectric states (Table 2). Bearing in mind that a comparison of the effects that have different physical natures and are caused by different fields is fairly subjective, it should be noted, nonetheless, that the magnitudes of ΔT_{AD} and ΔS_{PCE} for the oxyfluorides are at the level of the most significant caloric effects.

5. CONCLUSIONS

The performed studies of the thermal expansion allowed us to extend the notions of the features of the mechanism of the structural transformations in $(NH_4)_2WO_2F_4$ and $(NH_4)_2MoO_2F_4$ and to establish the correlation between the behavior of the volume and linear thermal expansion coefficients and the heat capacity over wide temperature ranges below T_1 and T_2. The analysis of the data in terms of the Pippard relations made it possible to determine the pressure coefficients dT/dp and $dT/d\sigma$ and to construct the total p–T and σ–T phase diagrams, which indicate the direction (in the crystals) responsible for the significant differences between the values of dT_1/dp. It was established that, in the molybdate, in contrast to the tungstate, the range of stability of the intermediate distorted phase increases under pressure.

It was revealed that, in the $(NH_4)_2MoO_2F_4$ oxyfluoride undergoing two phase transitions, one of which at T_1 is the order–disorder transition, the hydrostatic pressure and uniaxial stress along the b direction induce fairly strong intensive and extensive barocaloric effects comparable in magnitude to the caloric effects observed in a number of magnets and ferroelectrics. The performed studies allowed the conclusion that the external pressure is a fairly effective tool for changing the entropy of compounds that contain ordering ions or ionic groups. It is quite probable that, apart from ferroelectric and magnetic materials, in which the caloric effects are induced by electric and magnetic fields, attention of researchers will be attracted to ferroelastics and materials with a mixed nature, such as ferroelectromagnets–ferroelastics, ferroelectrics–ferroelastics, etc., in which significant caloric effects can be induced by the hydrostatic or uniaxial pressure.

ACKNOWLEDGMENTS

This study was performed within the framework of the Interdisciplinary Integration Project no. 34 of the Siberian Branch of the Russian Academy of Sciences and supported by the Krasnoyarsk Regional Science Foundation and the Russian Foundation for Basic Research within the framework of the project "Sibir'" (grant no. 09-02-98001) and by the Council on Grants from the President of the Russian Federation for the Support of Leading Scientific Schools (project no. NSh-1011.2008.2).

REFERENCES

1. K. R. Heier, A. J. Norquist, P. S. Halasyamani, A. Duarte, C. L. Stern, and K. R. Poeppelmeier, Inorg. Chem. **38**, 762 (1999).
2. K. R. Heier, A. J. Norquist, C. G. Wilson, C. L. Stern, and K. R. Poeppelmeier, Inorg. Chem. **37**, 76 (1998).
3. M. Vlasse, J.-M. Moutou, M. Cervera-Marzal, J.-P. Chaminade, and P. Hagenmüller, Rev. Chim. Miner. **19**, 58 (1982).
4. G. Z. Pinsker and V. G. Kuznetsov, Kristallografiya **13** (1), 74 (1968) [Sov. Phys. Crystallogr. **13** (1), 56 (1968)].
5. V. S. Sergienko, M. P. Poraĭ-Koshits, and T. S. Khodashova, Zh. Strukt. Khim. **13** (3), 461 (1972).
6. A. M. Srivastava and J. E. Ackerman, J. Solid State Chem. **98**, 144 (1992).
7. A. A. Udovenko and N. M. Laptash, Acta Crystallogr., Sect. B: Struct. Sci. **64**, 645 (2008).
8. S. V. Mel'nikova, V. D. Fokina, and N. M. Laptash, Fiz. Tverd. Tela (St. Petersburg) **48** (1), 110 (2006) [Phys. Solid State **48** (1), 117 (2006)].
9. I. N. Flerov, V. D. Fokina, M. V. Gorev, A. D. Vasiliev, A. F. Bovina, M. S. Molokeev, A. G. Kocharova, and N. M. Laptash, Fiz. Tverd. Tela (St. Petersburg) **48** (4), 711 (2006) [Phys. Solid State **48** (4), 759 (2006)].
10. A. D. Vasiliev and N. M. Laptash, in *Proceedings of the Third International Workshop on Advanced Inorganic Fluorides (ISIF-2008), Vladivostok, Russia, 2008* (Vladivostok, 2008), p. 187.
11. I. N. Flerov, V. D. Fokina, A. F. Bovina, E. V. Bogdanov, M. S. Molokeev, A. G. Kocharova, E. I. Pogorel'tsev, and N. M. Laptash, Fiz. Tverd. Tela (St. Petersburg) **50** (3), 497 (2008) [Phys. Solid State **50** (3), 515 (2008)].
12. I. N. Flerov, V. D. Fokina, M. V. Gorev, E. V. Bogdanov, M. S. Molokeev, A. F. Bovina, and A. G. Kocharova, Fiz. Tverd. Tela (St. Petersburg) **49** (6), 1093 (2007) [Phys. Solid State **49** (6), 1149 (2007)].
13. S. V. Mel'nikova and N. M. Laptash, Fiz. Tverd. Tela (St. Petersburg) **50** (3), 493 (2008) [Phys. Solid State **50** (3), 511 (2008)].
14. S. V. Mel'nikova, A. D. Vasil'ev, and N. M. Laptash, in *Proceedings of the 10th International Symposium "Order, Disorder, and Properties of Oxides" (ODPO-10), Loo, Krasnodar region, Russia, 2007* (Polytechnical Institute of the Southern Federal University, Rostov-on-Don, 2007), Part II, p. 172.
15. V. D. Fokina, E. V. Bogdanov, E. I. Pogorel'tsev, V. S. Bondarev, I. N. Flerov, and N. M. Laptash, Fiz. Tverd. Tela (St. Petersburg) **52** (1), 148 (2010) [Phys. Solid State **52** (1), 158 (2010)].
16. A. M. Tishin and Y. I. Spichkin, *The Magnetocaloric Effect and Its Applications* in *Series in Condensed Matter Physics* (Institute of Physics, Bristol, United Kingdom, 2003).
17. J. F. Scott, Science (Washington) **315**, 954 (2007).
18. K. A. Müller, F. Fauth, S. Fischer, M. Koch, A. Furrer, and Ph. Lacorre, Appl. Phys. Lett. **73**, 1056 (1998).
19. Th. Strässle, A. Furrer, A. Donni, and T. Komatsubara, J. Appl. Phys. **91**, 8543 (2002).
20. Th. Strässle, A. Furrer, Z. Hossain, and Ch. Geibel, Phys. Rev. B: Condens. Matter **67**, 054 407 (2003).
21. L. G. de Medeiros, N. A. de Oliveira, and A. Troper, J. Appl. Phys. **103**, 113909 (2008).
22. N. A. de Oliveira, J. Phys.: Condens. Matter **20**, 175 209 (2008).
23. E. Bonnot, R. Romero, L. Manosa, E. Vives, and A. Planes, arXiv:0802.2009vl [cond-mat.mtrl-sci].
24. A. B. Pippard, *The Elements of Classical Thermodynamics* (Cambridge University Press, New York, 1964).
25. K. A. Gschneidner, Jr., V. K. Pecharsky, A. O. Pecharsky, V. V. Ivtchenko, and E. M. Levin, J. Alloys Compd. **303–304**, 214 (2000).
26. L. Shebanov, K. Borman, W. N. Lawless, and A. Kalvane, Ferroelectrics **273**, 137 (2002).
27. A. S. Mischenko, Q. Zhang, J. F. Scott, R. W. Whatmore, and N. D. Mathur, Science (Washington) **311**, 1270 (2006).

Translated by Yu. Ryzhkov